

Synergy of carbanion siting and hydrogen bonding in Super-nucleophilic deep eutectic solvents for efficient CO₂ capture

Meisi Chen¹, Wenjie Xiong², Shangyu Li¹, Weida Chen¹, Feng Zhang³, and Youting Wu²

¹Affiliation not available

²Nanjing University

³nanjing university

July 8, 2023

Abstract

Carbanion-based ionic liquids are proposed and utilized as the key components for the construction of five super-nucleophilic deep eutectic solvents (SNDESs) in the paper. The super-nucleophilic nature of carbanion-based ILs is found to enable the capture of CO₂ with large absorption capacity. However, the absorption is very slow in the IL due to high viscosity. The synergy of carbanion siting and hydrogen bonding is found to enable high and fast absorption of CO₂ in [N₂₂₂₂][CH(CN)₂]-ethylimidazole (Eim), and a synergistic absorption mechanism is proposed and validated from spectroscopic analyses and quantum calculations. The enthalpy change of CO₂ absorption in [N₂₂₂₂][CH(CN)₂]-Eim is calculated to be -39.6 kJ/mol according to the thermodynamic model, and the moderate value implies that both absorption and desorption of CO₂ in the DES are favored and well balanced. The synergism of carbanion and hydrogen bond mediated by SNDESs provides a novel insight into the efficient CO₂ capture.

1. INTRODUCTION

Carbon dioxide (CO₂) is known as the main cause of global warming^{1,2}, and the key to mitigating climate change is to cut off or capture its emission^{3,4}. It remains a challenge to capture CO₂ in a more effective and energy-efficient way⁵, and one common thought within the industry is to develop new agents to facilitate the process of CO₂ capture⁶⁻⁸. Since specific ionic liquids (ILs) were validated as ideal CO₂ capture agents⁹ in 1999, ILs have become a focused research field in gas capture because of their unique characteristics¹⁰, such as negligible vapor pressure¹¹, wide-range temperature steadiness, low corrosiveness¹² and physicochemical adjustability¹³⁻¹⁵.

Davis and his coworkers reported the first example of CO₂ chemisorption using amino-functionalized ILs in their work¹⁶. More amino-functional ILs were reported recently^{17,18}, such as imidazolium-based¹⁹, amino acid-based²⁰ and choline-based ILs²¹. ILs with oxygen-containing functional groups have also attracted interests among the fields²², and some ILs with aldehydes and phenolic compounds as anions have been developed successively to possess a fairly good solubility of CO₂²³. To the best of our knowledge, Dai group²⁴ reported the first and only example of using supernucleophilic carbanion as the interacting site of CO₂ in November 2022. Malononitrile is deprotonated to be the carbanion in their paper, and the ILs so derived have a maximum CO₂ uptake of 2.65 mol/kg at 298.2 K and 1.0 bar, close to the equimolar absorption of CO₂. In fact, before the publication of Dai's paper we had also been working on carbanion-based ILs using malononitrile as the starting material for more than four months. Even though the cations of our carbanion-based ILs are different, a similar absorption mechanism exists as in Dai's work. However, the carbanion-based ILs are found to have large viscosities, especially during the absorption of CO₂. The absorption of CO₂ is also quite slow due to the high viscosity^{25,26} and the ILs after absorption turn into gel

at 1.0 bar, suggesting that the pure carbanion-based ILs are not practical as absorbents, even though they have the excellent absorption mechanism resulting from the supernucleophilic nature of carbanion site.

As an environmental benign analogue of ILs, deep eutectic solvents (DESs) can overcome the shortcomings of ILs due to the presence of nonionic components in DESs^{27,28}. To date, more DESs with N and/or O as the interacting site(s) for CO₂ have been reported^{29,30}. Among them, Yan et al. reported that [HDBU][Im]/ethylene glycol (EG) with a molar ratio of 7:3 had a CO₂ uptake of 3.2 mol/kg at 313.2 K and 1.0 bar, and demonstrated that the absorption process in [HDBU][Im]/EG has a synergistic action of N and O sites, producing a mixture of carbamate and carbonate products³¹. In comparison with monoethanolamine (MEA) and ethylenediamine (EDA)³², the desorption of CO₂ from [HDBU][Im]/EG is superior although the absorption capacity is slightly lower. The efforts above demonstrate that DESs have their own extraordinary features, such as negligible volatility³³, high CO₂ affinity³⁴, low viscosity^{35,36}, and biocompatibility³⁷ owing to their unique hydrogen bonding network structure³⁸. Hence the question is, can the carbanion-based ILs be developed into carbanion-based DESs for efficient CO₂ capture? The answer is positive.

In this paper, a promising energy-efficient CO₂ capture system is proposed using carbanion-based ILs for the construction of DESs. The essence of our strategy is to exploit the supernucleophilic nature of carbanion for siting and attaching to CO₂, and the rich hydrogen bonding network in the DESs for easy stabling and decomposing of DES-CO₂ adducts, so that fast and high absorption/desorption of CO₂ can be realized in an energy-saving manner.

2. EXPERIMENTAL AND METHODOLOGY

2.1 Materials

CO₂ (99.99 mol%) was purchased from Nanjing Chuangda Gas Co., Ltd, China. Tetraethylammonium hydroxide ([N₂₂₂₂][OH], 25 wt% in methanol), Tetramethylammonium hydroxide ([N₁₁₁₁][OH], 25 wt% in methanol), malononitrile (CH₂(CN)₂, 99 wt%), and methanol (99.5 wt%) were supplied from Aladdin Chemical Reagent Co., Ltd. Ethylene glycol, (EG, 99 wt%), imidazole (Im, 99 wt%), 1-Ethylimidazole (Eim, 99 wt%), dimethyl-2-(2-aminoethoxy)ethanol (DMEE, 99wt%), Tetramethylene sulfone (SUL, 99 wt%), were purchased from Shanghai Macklin Biochemical Co., Ltd. All the chemicals were used directly without further purification.

2.2 Synthesis of SNDESs and Characterization

The [N₂₂₂₂][CH(CN)₂] and [N₁₁₁₁][CH(CN)₂] were synthesised by a two-step method. Initially, a 25 wt% methanolic solution of malononitrile (1.5 equiv) was gradually added to a 25 wt % methanolic solution of [N₂₂₂₂][OH] (1 equiv) under ice bath conditions and stirred for 1 h. The temperature was then raised to 323.2 K and stirring continued for an additional 8 hours. The orange-red liquid was obtained by spin evaporation at 323.2 K for 0.5 h, and the orange-red liquid along with excess ether was placed in a separatory funnel. The lower liquid layer was extracted by spin evaporation to yield a reddish-brown liquid, which was characterized by NMR and FT-IR to confirm the formation of the desired product, [N₂₂₂₂][CH(CN)₂]. The preparation of [N₁₁₁₁][CH(CN)₂] was carried out as above.

Five DESs, including [N₂₂₂₂][CH(CN)₂]-EG (1:1), [N₂₂₂₂][CH(CN)₂]-Im (1:1), [N₂₂₂₂][CH(CN)₂]-SUL (1:1), [N₂₂₂₂][CH(CN)₂]-DMEE (1:1) and [N₂₂₂₂][CH(CN)₂]-Eim (1:1). [N₂₂₂₂][CH(CN)₂] was mixed with each of the five HBDs at a molar ratio of 1:1 at 323.2 K until homogeneous liquids were obtained. The viscosities of five DESs based on [N₂₂₂₂][CH(CN)₂] were measured on a Brookfield LVDV-II + Pro viscometer from 303.2~333.2 K with a relative deviation of 1%.

2.3 Evaluation of SNDESs

The CO₂ loading of SNDESs was determined by dual-vessel absorption system as shown in **Figure S1**. The enthalpy change of system was estimated according to a previously used method, which is explained in the **Supporting Information**. Gaussian 09 program was performed to elucidate the molecular interaction between SNDESs and CO₂. All the geometries were fully optimized by the B3LYP method based on the density

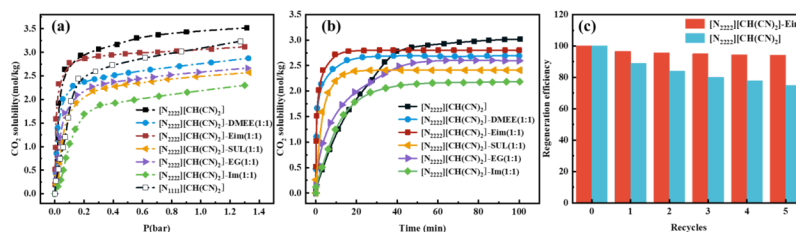
functional theory (DFT) including the dispersion corrections using the Empirical Dispersion=GD3BJ keyword. The influence of the solvent was investigated in the condensed phase using the Polarizable Continuum Model (PCM) with a dielectric constant of 24.55 at the B3LYP/6-311++g(d,p) level³⁹.

3.2 RESULTS AND DISCUSSION

3.1 CO₂ Capture Performance and Regeneration

The equilibrium absorption of CO₂ in carbanion-based ILs and DESs was first investigated as a function of partial pressure and is shown in **Figure 1a** (the detailed solubility data are given in **Table S1**). The same methodology as in our previous work was used for the measurements^{20,40,41}. In general, the basicity of a species has a positive influence on its uptake of CO₂. Due to the fact that [CH(CN)₂]⁻ is the supernucleophilic anion with high basicity (pKa=11)²⁴, the two ILs, [N₂₂₂₂][CH(CN)₂] and [N₁₁₁₁][CH(CN)₂], are endowed with high absorption capacities as expected (3.44 and 3.07 mol/kg at 303.2 K and 1.0 bar, respectively). [N₂₂₂₂][CH(CN)₂] has an apparently larger uptake of CO₂ than [N₁₁₁₁][CH(CN)₂], primarily due to the fact that the larger spatial structure of [N₂₂₂₂]⁺ cation provides more free volume for the accommodation of CO₂.⁴² However, when an even larger cation such as [P₆₆₆₁₄]⁺ is used, the absolute absorption of CO₂ in [P₆₆₆₁₄][CH(CN)₂] decreases to 2.65 mol/kg²⁴, even though equimolar absorption (a relative value) is approximately realized. It demonstrates that the cation has also an important influence on the absorption of CO₂ in the carbanion-based ILs, and that [N₂₂₂₂]⁺ is better than [P₆₆₆₁₄]⁺ and [N₁₁₁₁]⁺ in improving the absolute solubility.

In comparison with the carbanion-based ILs, the five carbanion-based DESs behave quite differently in the absorption of CO₂, and the nonionic components paired with [N₂₂₂₂][CH(CN)₂] in the DESs play the key roles. 1-ethylimidazole (Eim), as the hydrogen-bond acceptor (HBD) of weak basicity (pKa=7.1), enables the best absorption of CO₂ in [N₂₂₂₂][CH(CN)₂]-Eim (3.06 mol/kg at 1.0 bar and 303.2 K), whereas imidazole (Im), as the species of both acidity and basicity, behaves the worst in absorbing CO₂ into [N₂₂₂₂][CH(CN)₂]-Im (2.19 mol/kg). 2-(2-dimethylamino-ethoxy)-ethanol (DMEE) is the tertiary amine (pKa=8.95) that can assist [N₂₂₂₂][CH(CN)₂] to absorb CO₂ satisfactorily (2.77 mol/kg), better than the two neutral species, ethylene glycol (EG) and sulfolane (SUL), in the absorption (2.59 and 2.50 mol/kg). The uptakes of CO₂ in the five DESs follows the order of Eim>DMEE>EG>SUL>Im that cannot be interpreted only from the basicity of the nonionic components.



In general, the presence of nonionic components in the DESs usually leads to the decrease in the solubility of CO₂ due to the dilution effect, e.g., the uptake of CO₂ (3.44 mol/kg) in pure [N₂₂₂₂][CH(CN)₂] at 1.0 bar is larger than those in the five DESs (2.19 to 3.06 mol/kg). However, when the partial pressure is lower than 0.15 bar, it is interestingly noted that the absolute absorption of CO₂ in [N₂₂₂₂][CH(CN)₂]-Eim is even slightly larger than that in pure [N₂₂₂₂][CH(CN)₂]. In addition, when the partial pressure exceeds 0.2 bar, the absorption of CO₂ in [N₂₂₂₂][CH(CN)₂]-Eim levels off with the pressure, in contrary to the continuing absorption behavior of the pure IL. The two facts above imply that [N₂₂₂₂][CH(CN)₂], as the main absorbent in the DES, can react more efficiently with CO₂ at low pressures (<0.15 bar) under the assistance of Eim. It is deduced that the efficient chemical absorption at low pressures may be due to the cooperative interactions among [N₂₂₂₂][CH(CN)₂], CO₂, and Eim, that requires careful investigation. It should be also pointed out

that the DES $[N_{2222}][CH(CN)_2]$ -Eim is particularly suitable for the capture of CO_2 from flue gas due to its efficient chemical absorption at low partial pressures³⁸.

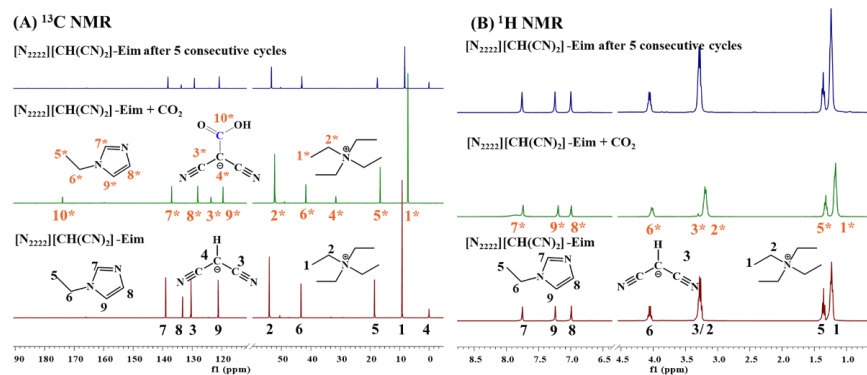
FIGURE 1. (a) Solubility of CO_2 in $[N_{1111}][CH(CN)_2]$, $[N_{2222}][CH(CN)_2]$ and $[N_{2222}][CH(CN)_2]$ -based DESs as a function of pressure at 303.2 K; (b) Dynamic absorption of CO_2 under 1.0 bar of initial pressure and 303.2 K; (c) Five consecutive cycles of CO_2 absorption/desorption in $[N_{2222}][CH(CN)_2]$ and $[N_{2222}][CH(CN)_2]$ -Eim (absorption under 1.0 bar and 303.2 K, and desorption under 0.025 bar and 353.2 K).

The dynamic absorption of CO_2 in the ILs and DESs is also investigated under 1.0 bar of initial pressure, 303.2 K, and constant gas-liquid area (**Figure 1b**, the detailed solubility data are given in **Table S2**). Impressively, the three Eim-, DMEE-, and SUL-based DESs, absorb CO_2 quite faster (<20 min to reach absorption equilibrium) than the pure IL $[N_{2222}][CH(CN)_2]$ (>70 min to reach equilibrium), and other two EG- and Im-based DESs (>50 min to reach equilibrium). In particular, the initial apparent absorption rate constant, K , in $[N_{2222}][CH(CN)_2]$ -Eim is calculated to be the largest, about 9 times of that in $[N_{2222}][CH(CN)_2]$ (2.35 vs. 0.26 min^{-1} , see **Table S3**), and about 18% and 56% larger than those in $[N_{2222}][CH(CN)_2]$ -DMEE and $[N_{2222}][CH(CN)_2]$ -SUL, respectively (2.35 vs. 1.99 and 1.5 min^{-1}). It indicates again that the cooperative chemical interactions exist in $[N_{2222}][CH(CN)_2]$ -Eim- CO_2 . It is reasonable to postulate that Eim as a special hydrogen bond acceptor (HBA) can stabilize the system by extending the hydrogen bond network of the DES to include CO_2 .

In fact, the absorption rate is greatly influenced by the solubility of CO_2 and the viscosity of absorbents. The larger solubility of CO_2 can provide a better concentration difference to drive the dynamic absorption, and this can be used to explain the absorption rates in the DESs decreasing in the order of Eim>DMEE>SUL>Im (3.06, 2.77, 2.50, and 2.19 mol/kg corresponding to K values of 2.35, 1.99, 1.5 and 0.42 min^{-1}). However, when the solubilities of CO_2 in $[N_{2222}][CH(CN)_2]$ -SUL and $[N_{2222}][CH(CN)_2]$ -EG differ very little (2.50 vs. 2.59 mol/kg), the larger absorption rate in the former DES than that in the latter (1.50 vs. 0.61 min^{-1}) has to be attributed to the smaller viscosity of the former DES (16.8 vs. 21.0 mPa·s). It should be particularly pointed out that the influence of viscosity on the rate prevails mainly during the absorption. At the beginning of the absorption, the pure IL and all DESs have in general small viscosities ranging from 27.6 to 12.7 mPa·s (see **Table S3**). However, the viscosity in the pure IL $[N_{2222}][CH(CN)_2]$ increases very fast during the absorption so that a very high viscosity value (5023 mPa·s at 303.2 K) is obtained at the end of the absorption (see **Table S4**). Even though the elevation of temperature can dramatically lower the solution viscosities (**Figure S2 and Table S4**), the fast increase in the viscosity during the absorption is still a problem, i.e., the viscosity rises still from 13.6 to 575.6 mPa·s at the temperature as high as 333.2 K. This is why the absorption rate in $[N_{2222}][CH(CN)_2]$ is the lowest in comparison with those in all DESs, even though $[N_{2222}][CH(CN)_2]$ has the largest solubility of CO_2 . In contrary, the viscosities of $[N_{2222}][CH(CN)_2]$ -Eim before and after absorption are 12.7 and only 115.7 mPa·s at 303.2 K, and 5.5 and only 24.4 mPa·s at 333.2 K (**Table S4**), justifying the fastest absorption rate in $[N_{2222}][CH(CN)_2]$ -Eim due to the lowest viscosity.

Multiple cycles of CO_2 absorption (under 1.0 bar and 303.2 K) and desorption (under 0.025 bar and 353.2 K) in $[N_{2222}][CH(CN)_2]$ and $[N_{2222}][CH(CN)_2]$ -Eim are investigated as examples to show the reversibility or recyclability of the absorbents (**Figure 1c**, the detailed data are given in **Table S5**). Since the viscosity of $[N_{2222}][CH(CN)_2]$ after absorbing CO_2 is as high as 5023 mPa·s, the desorption of CO_2 is difficult, and the regeneration efficiency decreases gradually with the number of cycles, so that the absorption capacity after 5 cycles is only about 80% of its original value. As a comparison, the regeneration of $[N_{2222}][CH(CN)_2]$ -Eim is much easy, and the absorption capacity in each cycle keeps nearly constant at about 92% of the primitive. The majority of 8% of capacity loss occurs in the first cycle, mainly due to the incomplete desorption of CO_2 under the given conditions. In general, $[N_{2222}][CH(CN)_2]$ -Eim has high regeneration efficiency and excellent reversibility, much better than the pure IL.

3.2 Mechanism Analysis



To look into the different underlying mechanism of CO_2 absorption in $[\text{N}_{2222}][\text{CH}(\text{CN})_2]\text{-Eim}$ from that in the pure IL, NMR and FTIR analyses are done and given in **Figures 2, 3 and S3-S5**. It can be seen from **Figure 2A** that a new signal appears at 173.9 ppm (peak 10*) after CO_2 chemisorption, and the signals of two carbons in the anion $[\text{CH}(\text{CN})_2]^-$ shift downfield from -0.0002 to 31.5 ppm (peak 4*) and upfield from 133.3 to 123.6 ppm (peak 3*), respectively. Such signal changes in the DES are nearly the same as those in the pure IL (**Figures S3 and S4**), both indicating the formation of a new species, $[\text{C}(\text{CN})_2]\text{-COOH}$, from the adduction of CO_2 with the anion,^[14] However, the carbon signals in Eim all shift upfield after CO_2 absorption, especially the three aromatic carbons of Eim (peaks 7* to 9*). In addition, it is shown in ^1H NMR (**Figure 2B**) that hydrogens 5* to 9* are also all shift upfield. In particular, hydrogen 7* has the tendency of forming two adjacent signal peaks. All the observations above implies the active participation of Eim in the reaction of CO_2 with $[\text{N}_{2222}][\text{CH}(\text{CN})_2]$. It is deduced that Eim participates the reaction probably via forming hydrogen bonds with $[\text{CH}(\text{CN})_2]\text{-CO}_2$ adduct, since the acidic hydrogen 7 and its adjacent alkaline nitrogen of Eim are hydrogen bond donor and acceptor, respectively. It is interestingly noted that a weak peak appears at 3.3 ppm in the ^1H -NMR spectra of samples after CO_2 absorption. It should be assigned to the hydrogen in $[\text{CH}(\text{CN})_2]^-$, due to the fact that the signal peak 2 masks peak 3 in the fresh $[\text{N}_{2222}][\text{CH}(\text{CN})_2]\text{-Eim}$ and the hydrogen in the samples in use or after use is detectable again as a weak signal when peak 2 moves slightly its location. The conclusion is also supported indirectly from the ^{13}C NMR of $[\text{N}_{2222}][\text{CH}(\text{CN})_2]\text{-Eim}$, where no impurity carbon signals are visible even after 5 cycles of use.

FIGURE 2. (A) ^{13}C NMR spectra (CDCl_3 in capillary tubes, 101 MHz) of $[\text{N}_{2222}][\text{CH}(\text{CN})_2]$ before and after CO_2 absorption; (B) ^1H NMR spectra (CDCl_3 in capillary tubes, 400 MHz) of $[\text{N}_{2222}][\text{CH}(\text{CN})_2]\text{-Eim}$ before and after CO_2 absorption.

In FTIR spectra (**Figure 3**), two characteristic peaks at 1621 cm^{-1} and 1286 cm^{-1} are dramatically strengthened after the saturation of CO_2 , evidenced as the stretching vibrations of $\text{C}=\text{O}$ and $\text{C}-\text{O}$ groups in the species $[\text{C}(\text{CN})_2]\text{-COOH}$. The two peaks exist also in the FTIR of fresh sample as very weak signals, primarily due to the slight uptake of CO_2 from the air during the offline FTIR analysis. The existence of COOH group can also be evidenced from the two broad and weak peaks at 2700 to 2500 cm^{-1} that originate from the frequency combination of $\text{C}=\text{O}$ stretching with $\text{O}-\text{H}$ bending and the frequency doubling of $\text{C}-\text{O}$ stretching. Another very important information is the two peaks of $-\text{C}[\text{?}]\text{N}$ that shift from 2104 to 2160 cm^{-1} and from 2156 to 2195 cm^{-1} after the absorption of CO_2 . There is also a peak at 2077 cm^{-1} disappearing after CO_2 absorption, probably due to the fade of $\text{C}=\text{C}=\text{N}$ stretching when CO_2 is inserted into the anion $[\text{CH}(\text{CN})_2]^-$. The FTIR analysis above is in consistence with the NMR results, confirming the formation of $[\text{C}(\text{CN})_2]\text{-COOH}$.

Hosted file

image3.emf available at <https://authorea.com/users/342837/articles/653633-synergy-of-carbanion-siting-and-hydrogen-bonding-in-super-nucleophilic-deep-eutectic-solvents-for-efficient-co2-capture>

FIGURE 3. FTIR spectra of $[\text{N}_{2222}][\text{CH}(\text{CN})_2]$ -Eim before and after CO_2 absorption

3.3 Thermodynamics and Enthalpy Change Estimation.

The enthalpy change, ΔH , is investigated from the effect of temperature on the absorption of CO_2 in $[\text{N}_{2222}][\text{CH}(\text{CN})_2]$ -Eim and $[\text{N}_{2222}][\text{CH}(\text{CN})_2]$. The solubility of CO_2 in the DES or in the IL is determined and found to decrease with the increasing temperature (**Figure 4a, b**, the detailed solubility data are given in **Table S6-7**), in consistence with the fact that the chemical absorption of CO_2 is exothermic^{43,44}. With the assumption of equimolar reaction of CO_2 with the DES or IL (supported by the NMR and FTIR results), a reactive phase equilibrium model (RPEM) is developed to fit the experimental solubility of CO_2 (see **Supporting Information** for model derivation). The model represents the experimental data quite well (see lines in **Figure 4a, b**), and ΔH is calculated to be -39.6 kJ/mol in the DES and -41.8 kJ/mol in the IL (**Figure S6**). The experimental enthalpy change of -41.8 kJ/mol in $[\text{N}_{2222}][\text{CH}(\text{CN})_2]$ is slightly more negative than the theoretical value of -35.33 kJ/mol in $[\text{P}_{66614}][\text{CH}(\text{CN})_2]$ calculated by Dai's group^[14], due to the differences in the cation of IL and also in the methodology of calculation. Nevertheless, the enthalpy changes both in the DES and IL are moderate, favoring both the absorption and desorption of CO_2 .

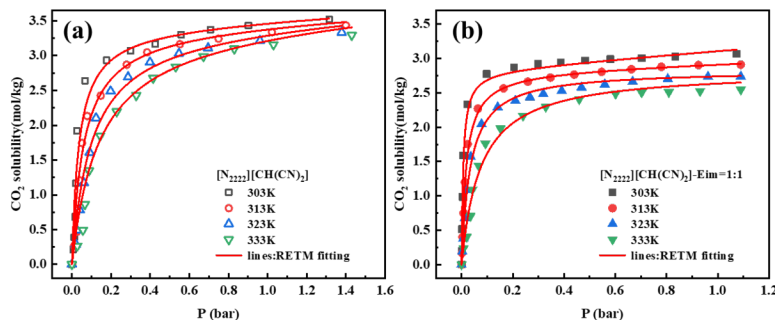


FIGURE 4. Absorption of CO_2 in (a) $[\text{N}_{2222}][\text{CH}(\text{CN})_2]$ and (b) $[\text{N}_{2222}][\text{CH}(\text{CN})_2]$ -Eim at different temperatures.

Combining all the results or information obtained, a plausible mechanism of CO_2 absorption in $[\text{N}_{2222}][\text{CH}(\text{CN})_2]$ -Eim is proposed and schematically given in **Figure 5** (the detailed data are given in **Table S8**). The mechanism is expressed as the synergy of carbanion siting for the insertion of CO_2 and hydrogen bonding for the stabilization of $[\text{CH}(\text{CN})_2]\text{-CO}_2\text{-Eim}$ complex. To further verify the mechanism, theoretical calculations are performed using the density functional theory (DFT) at the B3LYP/6-311++G(d, p) level.⁴⁵⁻⁴⁷ It is indicated from the optimized configurations (**Figure 5b**) that $[\text{C}(\text{CN})_2]\text{-COOH}$ is produced via the insertion of CO_2 into the carbanion site followed by the hydrogen transfer from the carbanion site to the oxygen site of CO_2 in the first stage. The central carbon of carbanion undergoes structural changes from sp^2 to sp^3 and finally back to sp^2 hybridization, and the carbon of CO_2 is also hybridized from sp to sp^2 in this stage, same as the finding by Dai and his coworker²⁴. However, due to the existence of Eim in the DES, $[\text{C}(\text{CN})_2]\text{-COOH}$ can be further stabilized through the formation of hydrogen bonding with Eim in the second stage (**Figure 5c**). A quasi-six-membered ring in the same plane is generated with the assistance of two intramolecular hydrogen bonds (bond lengths of $\text{H}_{\text{Eim}}\text{-O}_{\text{CO}_2}$ and H-N_{Eim} are 2.55 and 1.66 Å). The enthalpy change for the carbanion siting of CO_2 in the first stage is -29.6 kJ/mol, while the value under the synergy of carbanion siting and hydrogen binding is as negative as -68.3 kJ/mol. The energy change due to the formation of two intramolecular hydrogen bonds in the second stage is thus calculated to be -38.7 kJ/mol from the two data above, close to the value of -39.6 kJ/mol calculated from the experimental solubility of

CO₂. The synergistic mechanism of carbanion siting and hydrogen bonding reveals the feasibility of efficient CO₂ capture using carbanion-based DESs.

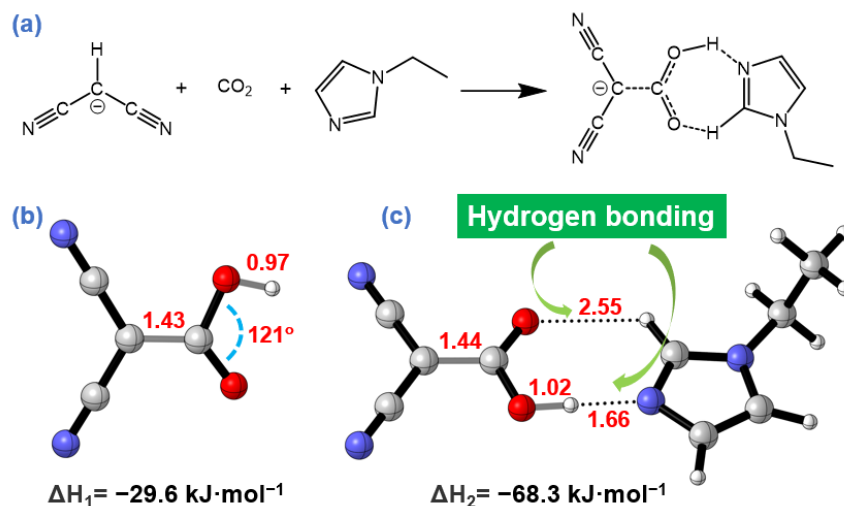


FIGURE 5. (a) Synergistic mechanism of carbanion siting and hydrogen bonding for CO₂ absorption in [N₂₂₂₂][CH(CN)₂]-Eim; (b) Optimized configuration of carbanion-CO₂ adduct; (c) Optimized configuration of carbanion-CO₂-Eim complex.

4. DATA AVAILABILITY AND REPRODUCIBILITY STATEMENT

The numerical data from Figures 1 and 4 are tabulated in the Supplementary Materials. Numerical data for the FTIR spectra from Figures 4 and source data of NMR for Figures 2 are available as .zip file in the Supplementary Material. For Gaussian calculations, these input files include complete information on the B3LYP/6-311++G (d, p) level and other simulation settings that were used in our Gaussian calculations.

Absolute deviation tabulated in Supplementary Materials from Figures 1a-1b and 4 show the spread of data observed in triplicate measurements, where independent samples were tested for each measurement.

5. CONCLUSIONS

A series of carbanion-based ILs and DESs are developed successfully in the paper for efficient capture of CO₂. The super-nucleophilic nature of carbanion favors the direct insertion of CO₂ to form carbanion-CO₂ adduct and enable high absorption capacities of ILs and DESs. In comparison with the pure ILs, the SNDESs are additionally featured with much low viscosity, fast absorption of CO₂, excellent recyclability, and abundant hydrogen bond interactions for the energy reduction during the absorption. In particular, the carbanion siting and hydrogen bonding can function synergistically in the absorption of CO₂ in [N₂₂₂₂][CH(CN)₂]-Eim, and the new absorption mechanism is verified from spectroscopic analyses together with thermodynamic and quantum calculations. The achievements made in this work provide an alternative design strategy of SNDESs, and the SNDESs are believed to have great potential in the applications of CO₂ capture.

AUTHOR CONTRIBUTIONS

Meisi Chen : Data curation (lead); formal analysis (lead); investigation (lead); methodology (lead); validation (lead); writing—original draft (lead). **Wenjie Xiong** : soft (lead); investigation (supporting); **Shangyu Li**: validation (supporting). Weida Chen: methodology (supporting). **Feng Zhang** : Conceptualization (equal); funding acquisition (supporting); methodology (lead); resources (supporting); supervision (equal); writing—review & editing (lead). **Youting Wu** : Conceptualization (lead); funding acquisition

(lead); methodology (lead); project administration (lead); supervision (lead); writing–review and editing (lead).

REFERENCES

1. Carneiro JSA, Innocenti G, Moon HJ, et al. Insights into the Oxidative Degradation Mechanism of Solid Amine Sorbents for CO₂ Capture from Air: Roles of Atmospheric Water. *Angewandte Chemie (International ed. in English)*. 2023-Apr-17 2023:e202302887-e202302887.
2. Liu J, Yang D, Zhou Y, et al. Tricycloquinazoline-Based 2D Conductive Metal-Organic Frameworks as Promising Electrocatalysts for CO₂ Reduction. *Angewandte Chemie-International Edition*. Jun 21 2021;60(26):14473-14479.
3. Ozkan M, Akhavi A-A, Coley WC, Shang R, Ma Y. Progress in carbon dioxide capture materials for deep decarbonization. *Chem.* Jan 13 2022;8(1):141-173.
4. Li C, Xiong W, Zhao T, et al. Mechanochemical construction of mesoporous silicon-supported organocatalysts with alkylol-amine cooperative sites for CO₂ fixation into cyclic carbonates under halogen-free conditions. *Appl. Catal. B: Environ.* 2023;324:122217.
5. Tan Z, Zhang S, Zhao F, et al. SnO₂/ATP catalyst enabling energy-efficient and green amine-based CO₂ capture. *Chemical Engineering Journal*. Feb 1 2023;453.
6. Qu K, Xu J, Dai L, et al. Electrostatic-Induced Crystal-Rearrangement of Porous Organic Cage Membrane for CO₂ Capture. *Angewandte Chemie-International Edition*. Aug 1 2022;61(31).
7. Meng F, Meng Y, Ju T, Han S, Lin L, Jiang J. Research progress of aqueous amine solution for CO₂ capture: A review. *Renewable & Sustainable Energy Reviews*. Oct 2022;168.
8. Zhou Y, Zhang JL, Wang L, et al. Self-assembled iron-containing mordenite monolith for carbon dioxide sieving. *Science*. Jul 2021;373(6552):315-+.
9. Blanchard LA, Hancu D, Beckman EJ, Brennecke JF. Green processing using ionic liquids and CO₂. *Nature*. May 6 1999;399(6731):28-29.
10. Avila J, Lepre LF, Santini CC, et al. High-Performance Porous Ionic Liquids for Low-Pressure CO₂ Capture**. *Angewandte Chemie-International Edition*. Jun 1 2021;60(23):12876-12882.
11. Cota I, Fernandez Martinez F. Recent advances in the synthesis and applications of metal organic frameworks doped with ionic liquids for CO₂ adsorption. *Coordination Chemistry Reviews*. 2017/11/15/2017;351:189-204.
12. Hernández E, Hospital-Benito D, Moya C, et al. Integrated carbon capture and utilization based on bifunctional ionic liquids to save energy and emissions. *Chemical Engineering Journal*. 2022/10/15/2022;446:137166.
13. Eshetu GG, Armand M, Scrosati B, Passerini S. Energy Storage Materials Synthesized from Ionic Liquids. *Angewandte Chemie-International Edition*. Dec 1 2014;53(49):13342-13359.
14. Zeng S, Zhang X, Bai L, et al. Ionic-Liquid-Based CO₂ Capture Systems: Structure, Interaction and Process. *Chemical Reviews*. Jul 26 2017;117(14):9625-9673.
15. Zhang X, Zhang X, Dong H, Zhao Z, Zhang S, Huang Y. Carbon capture with ionic liquids: overview and progress. *Energy & Environmental Science*. 2012;5(5):6668-6681.
16. Bates ED, Mayton RD, Ntai I, Davis JH. CO₂ capture by a task-specific ionic liquid. *Journal of the American Chemical Society*. Feb 13 2002;124(6):926-927.
17. Aghaie M, Rezaei N, Zendehboudi S. A systematic review on CO₂ capture with ionic liquids: Current status and future prospects. *Renewable & Sustainable Energy Reviews*. Nov 2018;96:502-525.

18. Raeisi M, Keshavarz A, Rahimpour MR. Ionic Liquids for Carbon Dioxide Capture. In: Inamuddin, Asiri AM, Lichtfouse E, eds. *Sustainable Agriculture Reviews 38: Carbon Sequestration Vol. 2 Materials and Chemical Methods*. Vol 382019:193-219.
19. Yin M, Wang L, Tang S. Amino-Functionalized Ionic-Liquid-Grafted Covalent Organic Frameworks for High-Efficiency CO₂ Capture and Conversion. *Acs Applied Materials & Interfaces*. 2022.
20. Chen M, Li M, Zhang L, Liu X, Zhang F, Wu Y. Intensification of Amino Acid Ionic Liquids with Different Additives for CO₂ Capture. *ACS Sustainable Chemistry & Engineering*. 2022/09/19 2022;10(37):12082-12089.
21. Ishak MAI, Jumbri K, Daud S, et al. Molecular simulation on the stability and adsorption properties of choline- based ionic liquids/IRMOF-1 hybrid composite for selective H₂S/CO₂ capture. *Journal of Hazardous Materials*. Nov 15 2020;399.
22. Sharma P, Choi S-H, Park S-D, Baek I-H, Lee G-S. Selective chemical separation of carbondioxide by ether functionalized imidazolium cation based ionic liquids. *Chemical Engineering Journal*. Feb 1 2012;181:834-841.
23. Chen Y, Qu Z, Hu H, Gao Y. Nonaqueous amino-phenolic dual-functionalized ionic liquid absorbents for reversible CO₂ capture: Phase change behaviors and mechanism. *Separation and Purification Technology*. 2023/03/01/ 2023;308:122986.
24. Suo X, Fu Y, Do-Thanh C-L, et al. CO₂ Chemisorption Behavior in Conjugated Carbanion-Derived Ionic Liquids via Carboxylic Acid Formation. *Journal of the American Chemical Society*. 2022.
25. Ma C, Wang N, Ye N, Ji X. CO₂ capture using ionic liquid-based hybrid solvents from experiment to process evaluation. *Applied Energy*. 2021/12/15/ 2021;304:117767.
26. Zhang Y, Ji X, Lu X. Choline-based deep eutectic solvents for CO₂ separation: Review and thermodynamic analysis. *Renewable & Sustainable Energy Reviews*. Dec 2018;97:436-455.
27. Pena CA, Soto A, Rodriguez H. Tetrabutylphosphonium acetate and its eutectic mixtures with common-cation halides as solvents for carbon dioxide capture. *Chemical Engineering Journal*. Apr 1 2021;409.
28. Sarmad S, Mikkola J-P, Ji X. Carbon Dioxide Capture with Ionic Liquids and Deep Eutectic Solvents: A New Generation of Sorbents. *Chemsuschem*. Jan 20 2017;10(2):324-352.
29. Yan H, Zhao L, Bai Y, et al. Superbase Ionic Liquid-Based Deep Eutectic Solvents for Improving CO₂ Absorption. *ACS Sustainable Chemistry & Engineering*. 2020;8(6):2523-2530.
30. Zhang C. Carbon dioxide capture: Multiple site absorption. *Nature Energy*. 2016/06/07 2016;1(6):16084.
31. Lee Y-Y, Penley D, Klemm A, Dean W, Gurkan B. Deep Eutectic Solvent Formed by Imidazolium Cyanopyrrolide and Ethylene Glycol for Reactive CO₂ Separations. *ACS Sustainable Chemistry & Engineering*. 2021/01/25 2021;9(3):1090-1098.
32. Trivedi TJ, Lee JH, Lee HJ, Jeong YK, Choi JW. Deep eutectic solvents as attractive media for CO₂ capture. *Green Chemistry*. 2016 2016;18(9):2834-2842.
33. Xiong W, Zhang X, Tu Z, Hu X, Wu Y. Novel Deep Eutectic Electrolyte Induced by Na...N Interactions for Sodium Batteries. *Ind. Eng. Chem. Res*. 2022/12/27 2023;62(1):51-61.
34. Lin H, Gong K, Ying W, et al. CO₂-Philic Separation Membrane: Deep Eutectic Solvent Filled Graphene Oxide Nanoslits. *Small*. Dec 6 2019;15(49).
35. Xiong W, Shi M, Peng L, Zhang X, Hu X, Wu Y. Low viscosity superbase protic ionic liquids for the highly efficient simultaneous removal of H₂S and CO₂ from CH₄. *Sep. Purif. Technol*. 2021;263:118417.

36. Xiong W, Lu Y, Li C, Geng J, Wu Y-T, Hu X. An Imidazole-based DES Serving as a “Courier” for the Efficient Coupling of HCl Capture and Conversion under Mild Conditions. *Green Chemistry*. 2023;DOI: 10.1039/D2GC03866H.
37. Lin H, Gong K, Hykys P, et al. Nanoconfined deep eutectic solvent in laminated MXene for efficient CO₂ separation. *Chemical Engineering Journal*. Feb 1 2021;405.
38. Sarmad S, Xie Y, Mikkola J-P, Ji X. Screening of deep eutectic solvents (DESs) as green CO₂ sorbents: from solubility to viscosity. *New Journal of Chemistry*. Jan 7 2017;41(1):290-301.
39. Frisch M, Trucks G, Schlegel H, et al. Gaussian 09 Revision A. 1, 2009. 2009;139.
40. Zhang X, Xiong W, Peng L, Wu Y, Hu X. Highly selective absorption separation of H₂S and CO₂ from CH₄ by novelazole-based protic ionic liquids. *AIChE J*. 2020;66(6):e16936.
41. Wu H, Xiong W, Wen S, Zhang X, Zhang S. Homologue-paired liquids as special non-ionic deep eutectic solvents for efficient absorption of SO₂. *Chem. Commun.* Jul 12 2022;58(56):7801-7804.
42. Chen LD. Cations play an essential role in CO₂ reduction. *Nature Catalysis*. Aug 2021;4(8):641-642.
43. Pandey D, Mondal MK. Thermodynamic modeling and new experimental CO₂ solubility into aqueous EAE and AEEA blend, heat of absorption, cyclic absorption capacity and desorption study for post-combustion CO₂ capture. *Chemical Engineering Journal*. Apr 15 2021;410.
44. Chen S, Han X, Sun X, Luo X, Liang Z. The comparative kinetics study of CO₂ absorption into non-aqueous DEEA/MEA and DMEA/MEA blended systems solution by using stopped-flow technique. *Chemical Engineering Journal*. Apr 15 2020;386.
45. Ji J, Xiong W, Zhang X, et al. Reversible absorption of NF₃ with high solubility in Lewis acidic ionic liquids. *Chem. Eng. J*. 2022;440:135902.
46. Xiong W, Shi M, Lu Y, et al. Efficient conversion of H₂S into mercaptan alcohol by tertiary-amine functionalized ionic liquids. *Chinese J. Chem. Eng.* 2022;50:197-204.
47. Xiong W, Shi M, Zhang X, Tu Z, Hu X, Wu Y. The efficient conversion of H₂S into mercaptan alcohols mediated in protic ionic liquids under mild conditions. *Green Chem.* 2021;23(20):7969-7975.